

# High speed, wide velocity dynamic range Doppler optical coherence tomography (Part III): *in vivo* endoscopic imaging of blood flow in the rat and human gastrointestinal tracts

Victor X.D. Yang<sup>3</sup>, Maggie L. Gordon<sup>3</sup>, Shou-jiang Tang<sup>1</sup>, Norman E. Marcon<sup>1</sup>,  
Geoffrey Gardiner<sup>2</sup>, Bing Qi<sup>5</sup>, Stuart Bisland<sup>3</sup>, Emily Seng-Yue<sup>5</sup>, Stewart Lo<sup>5</sup>,  
Julius Pekar<sup>5</sup>, Brian C. Wilson<sup>3,5,6</sup> and I. Alex Vitkin<sup>3,4,5</sup>

<sup>1</sup>Centre for Therapeutic Endoscopy and Endoscopic Oncology, and

<sup>2</sup>Dept. of Pathology, St. Michael's Hospital, Toronto, ON M5B 1W8, Canada

<sup>3</sup>Depts. of Medical Biophysics and <sup>4</sup>Radiation Oncology, University of Toronto, Toronto, ON M5G 2M9, Canada

<sup>5</sup>Ontario Cancer Institute/University Health Network, Toronto, ON M5G 2M9, Canada

<sup>6</sup>Biophotonics Facility, Photonics Research Ontario, Toronto, ON M5G 2M9, Canada

**Abstract:** We previously described a fiber based Doppler optical coherence tomography system [1] capable of imaging embryo cardiac blood flow at 4~16 frames per second with wide velocity dynamic range [2]. Coupling this system to a linear scanning fiber optical catheter design that minimizes friction and vibrations, we report here the initial results of *in vivo* endoscopic Doppler optical coherence tomography (EDOCT) imaging in normal rat and human esophagus. Microvascular flow in blood vessels less than 100  $\mu\text{m}$  diameter was detected using a combination of color-Doppler and velocity variance imaging modes, during clinical endoscopy using a mobile EDOCT system.

©2003 Optical Society of America

**OCIS codes:** (110.4500) Optical Coherence Tomography; (170.3880) Medical and biological imaging; (170.1650) Coherence imaging; (100.6950) Tomographic image processing

---

## References

1. V. X. Yang, M. L. Gordon, B. Qi, J. Pekar, S. Lo, E. Seng-Yue, A. Mok, B. C. Wilson, and I. A. Vitkin, "High speed, wide velocity dynamic range Doppler optical coherence tomography (Part I): System design, signal processing, and performance," *Opt. Express* **11**, 794-809 (2003), <http://www.opticsexpress.org/abstract.cfm?URI=OPEX-11-7-794>.
2. V. X. Yang, M. L. Gordon, E. Seng-Yue, S. Lo, B. Qi, J. Pekar, A. Mok, B. C. Wilson, and I. A. Vitkin, "High speed, wide velocity dynamic range Doppler optical coherence tomography (Part II): Imaging *in vivo* cardiac dynamics of *Xenopus laevis*," *Opt. Express* **11**, 1650-1658 (2003), <http://www.opticsexpress.org/abstract.cfm?URI=OPEX-11-14-1650>.
3. D. Huang, E. A. Swanson, C. P. Lin, J. S. Schuman, W. G. Stinson, W. Chang, M. R. Hee, T. Flotte, K. Gregory, C. A. Puliafito, and J. G. Fujimoto, "Optical coherence tomography," *Science* **254**, 1178-81 (1991).
4. G. J. Tearney, M. E. Brezinski, B. E. Bouma, S. A. Boppart, C. Pitris, J. F. Southern, and J. G. Fujimoto, "In vivo endoscopic optical biopsy with optical coherence tomography," *Science* **276**, 2037-9 (1997).
5. A. M. Rollins, R. Ung-arunyawee, A. Chak, R. C. K. Wong, K. Kobayashi, M. V. Sivak, Jr., and J. A. Izatt, "Real-time *in vivo* imaging of human gastrointestinal ultrastructure using endoscopic optical coherence tomography with a novel efficient interferometer design," *Opt. Lett.* **24**, 1358-60 (1999).
6. F. I. Feldchtein, G. V. Gelikonov, V. M. Gelikonov, R. V. Kuranov, A. M. Sergeev, N. Gladkova, A. V. Shakhov, N. M. Shakhova, L. B. Snopova, A. B. Terent'eva, E. V. Zagainova, Y. P. Chumakov, and I. A. Kuznetzova, "Endoscopic applications of optical coherence tomography," *Opt. Express* **3**, 257-70 (1998), <http://www.opticsexpress.org/abstract.cfm?URI=OPEX-3-6-257>.
7. B. E. Bouma and G. J. Tearney, "Power-efficient nonreciprocal interferometer and linear-scanning fiber-optic catheter for optical coherence tomography," *Opt. Lett.* **24**, 531-3 (1999).
8. J. M. Ponomeros, S. Brand, B. E. Bouma, G. J. Tearney, C. C. Compton, and N. S. Nishioka, "Diagnosis of specialized intestinal metaplasia by optical coherence tomography," *Gastroenterology* **120**, 7-12 (2001).
9. S. Yazdanfar, A. M. Rollins, and J. A. Izatt, "Imaging and velocimetry of the human retinal circulation with color Doppler optical coherence tomography," *Opt. Lett.* **25**, 1448-50 (2000).

10. Y. Zhao, Z. Chen, C. Saxer, S. Xiang, J. F. de Boer, and J. S. Nelson, "Phase-resolved optical coherence tomography and optical Doppler tomography for imaging blood flow in human skin with fast scanning speed and high velocity sensitivity," *Opt. Lett.* **25**, 114–116 (2000).
  11. X. Li, T. H. Ko, and J. G. Fujimoto, "Intraluminal fiber-optic Doppler imaging catheter for structural and functional optical coherence tomography," *Opt. Lett.* **26**, 1906-08 (2001).
  12. V. X. Yang, M. L. Gordon, A. Mok, Y. Zhao, Z. Chen, R. S. C. Cobbold, B. C. Wilson, I. A. Vitkin, "Improved phased-resolved optical Doppler tomography using the Kasai velocity estimator and histogram segmentation", *Opto. Commun.* **208**, 209-214, (2002).
  13. V. X. Yang, M. L. Gordon, B. Qi, E. S. Yue, S. Tang, S. K. Bisland, J. Pekar, S. Lo, N. E. Marcon, B. C. Wilson, and I. A. Vitkin, "High sensitivity detection and monitoring of microcirculation using cutaneous and catheter probes for Doppler optical coherence tomography," *Proc. SPIE* 4965, 153-159 (2003).
  14. V. X. Yang, B. Qi, M. L. Gordon, E. Seng-Yue, S. Tang, N. E. Marcon, I. A. Vitkin, B. C. Wilson, "In vivo feasibility of endoscopic catheter-based Doppler optical coherence tomography," *Digestive Disease Week Proceedings, Gastroenterology* **124**, Suppl.-1, A49 (2003).
  15. J.A.Jensen, *Estimation of blood velocities using ultrasound* (Cambridge, 1996).
  16. S. Yazdanfar, A. M. Rollins, and J. A. Izatt, "Ultra-high velocity resolution imaging of the microcirculation in vivo using color Doppler optical coherence tomography," *Proc. SPIE* 4251, 156-164 (2001).
- 

## 1. Introduction

Optical coherence tomography (OCT) [3] imaging of the gastrointestinal (GI) tract has been demonstrated by several groups using radial [4,5], lateral [6], or linear scanning catheter probes [7] to visualize subsurface tissue microstructure during endoscopy. An initial clinical study [8] suggested that rule-based criteria derived from the microstructural images might be useful for diagnosis of preneoplastic lesions in the human GI tract. Functional OCT imaging of the blood flow using Doppler techniques has been demonstrated in human retina and skin [9,10], showing initial potential for vascular diagnosis and treatment assessment under *in vivo* settings. The sample arm optics of these systems was, however, not catheter-based and so not amendable to endoscopic use. To date, only a flow phantom feasibility study of a radial scanning catheter for Doppler OCT has been reported [11]. Its scan geometry and velocity sensitivity (1–2 mm/s) made it more suitable for imaging in lumens with small diameter and high flow rate, such as the coronary artery. Larger diameter organs such as the GI tract are probably more accessible with the linear scanning catheter [7]. Adding Doppler capability to endoscopic OCT may allow detection of the vasculature associated with cancer or other pathological conditions, as well as monitoring of treatments that target the vasculature.

Extending the promising capability of Doppler OCT into endoscopic use is difficult. Firstly, the blood vessels within the penetration depth (1–2 mm) of OCT tend to be small (a few hundred  $\mu\text{m}$  in diameter), which contain slow moving (velocities of a few mm/s) red blood cells. Detecting such microvasculature requires a Doppler OCT system with high velocity sensitivity. Secondly, during endoscopy it is impossible to control the relative motion between the patient and the catheter tip. Motion artefacts caused by heart beat, breathing, muscle twitching, and GI tract peristalsis can overwhelm the true Doppler signal from the blood flow, since the velocity associated with these movements can be much higher than that of the red blood cells. Hence, a robust segmentation algorithm is required to remove the resulting motion artefacts. Finally, while the linear scanning catheter provides easier accessibility, its reciprocating motion induces more vibrations than the radial scanning probe's rotational motion, possibly increasing the background velocity noise level.

Our previous reports [1-2,12] addressed the first two issues. As the final paper of this series, we describe our approach to solve the last problem and demonstrate the feasibility of endoscopic Doppler OCT (EDOCT) imaging in both the rat and human GI tracts [13,14].

## 2. Material and methods

### 2.1 EDOCT system

The detail of our Doppler OCT system was described in the companion papers [1,2]. The system has been packaged into a mobile cart, similar to other groups conducting clinical OCT trials [5,8] for endoscopic use. This system conforms to the Canadian Standard Association's

medical equipment requirement for experimental patient use. The light source (JDS, Ottawa ON, Canada) provides a polarized output power of  $\sim 16$  mW at  $1.3 \mu\text{m}$  center wavelength with  $63$  nm of bandwidth, which allows an axial resolution of  $\sim 10 \mu\text{m}$  in tissue. The system uses a Michelson interferometer with an optical circulator and a rapid scanning optical delay (RSOD) operating at  $8$  kHz in the reference arm. The interferometer and the delay line are mounted on polyimide foam to reduce vibrations and improve phase stability. The foam is selected for its high acoustic absorption in the kHz range, which suppresses the  $8$  kHz audible noise for the clinical staff. The sample arm consists of a  $2$  mm outer diameter, side-viewing fiber optical catheter that fits through the accessory channel of a standard GI endoscope for clinical use. The details of this linearly scanning catheter are as follows.

## 2.2 Linear scanning catheter

The linear scanning motion of the catheter is produced by a galvanometer (Cambridge Technology, Cambridge, MA) which drives a piston using a connecting rod, as shown schematically in Fig. 1(a) and (b).

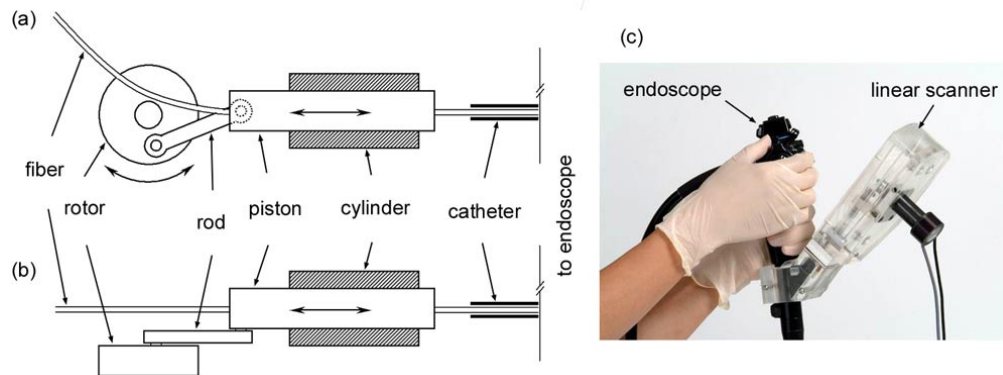


Fig. 1. Schematics of the mechanical assembly for the linear scanning catheter. (a) Top-view. (b) Side-view. This assembly is mounted on the endoscope, as shown in (c).

The stainless steel piston slides within a brass cylinder. Both are machined with high tolerance and lubricated to minimize friction or vibrations. Miniature ball bearings are integrated into the connecting rod, which connects the piston to the rotor of the galvanometer. The control loop of the galvanometer is electronically tuned to stably drive the entire mechanical assembly, which can move reciprocally over  $\sim 4$  mm (corresponding to  $\sim 40^\circ$  angular motion of the rotor) using a sinusoidal driving waveform up to  $\sim 150$  Hz. Through the center of the piston, a single mode optical fiber (SMF-28, cladding diameter =  $125 \mu\text{m}$ ) can be inserted and attached. This  $900 \mu\text{m}$  outer diameter fiber with plastic buffer slides within a  $2$ -mm outer diameter stationary guiding catheter (Wilson Cook, Winston Salem, NC). Both the fiber and guiding catheter can be rapidly removed and cleaned between patients. To further minimize friction, the sliding portion of the fiber is limited to the endoscope length by mounting the galvanometer assembly directly on the endoscope, over the accessory channel port, as shown in Fig. 1(c).

The galvanometer is driven by a modified saw-tooth waveform (see Fig. 2), provided by an arbitrary waveform generator (Agilent, Palo Alto, CA). The rising portion (part-1) of the waveform rapidly pushes the fiber towards the distal end of the catheter. The fast falling portion (part-2) initiates the pullback motion of the fiber, which is important for two reasons. The first is to restore tension quickly in the fiber at the beginning of the pullback motion, in order to counter the slack accumulated during the push-out motion. The second is to overcome the static friction between the fiber and the guiding catheter. Once the fiber starts sliding, the slow-falling portion (part-3) pulls the fiber back smoothly. The corners of the waveform are rounded to avoid vibrations. The distal tip of the fiber can be scanned using

this waveform at frequencies up to 30 Hz (the frequency component of the rising portion is less than 150 Hz). The scanning range (which is the lateral dimension of the field of view) is limited to 2 mm, in order to minimize the background noise in Doppler OCT imaging due to speckle modulation.

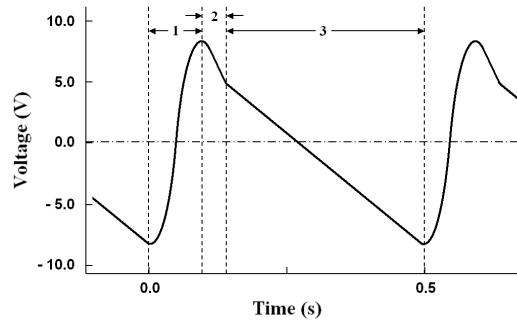


Fig. 2. Modified saw-tooth driving waveform for the linear scanning catheter. Part-1 pushes the fiber and part-2 starts the pullback motion. Images are acquired during the steady pullback motion of part-3.

The distal end of the optical fiber is terminated with 1 mm diameter, angle-polished, gradient-index (GRIN) lens and a 700  $\mu\text{m}$  aluminum-coated prism, both of which are aligned to the fiber using 1.1 mm outer diameter steel sheath. The surface of the steel sheath is polished to slide smoothly within either a slotted steel cap or a transparent plastic cover (Fig. 3), attached to the end of the guiding catheter. The advantage of the slotted cap is that the mucous layer can directly come into contact with the prism surface, thus serving as an index matching fluid between the optics and the intestinal wall. The disadvantage is that the cap blocks some of the radial viewing angles, so that the fiber must be rotated such that the imaging beam passes through one of the slots. In addition, the prism may drag the tissue if too much pressure is applied. The transparent cover design contains more reflecting interfaces between the prism and the tissue surface, which can increase the detected noise. Furthermore, it is difficult to insert index matching fluid between the prism and the cover without adverse effects such as friction or bubbling. The advantage of the transparent cover is that all radial angles are available for imaging. Both types were used in this work in an attempt to identify the superior functional design.

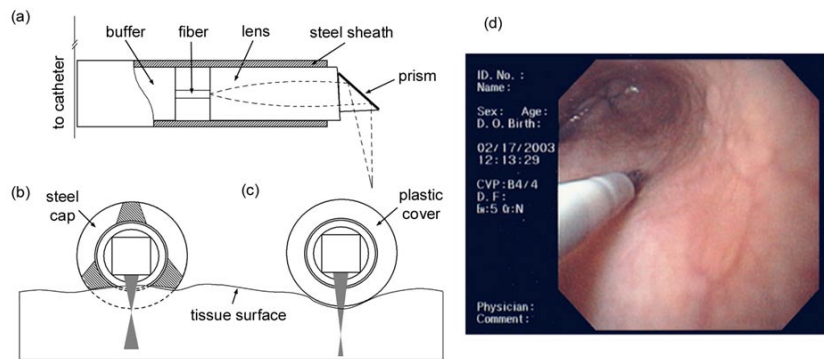


Fig. 3. Schematic of the EDOCT catheter distal end. (a) The fiber termination with GRIN lens and right-angle prism. The terminated fiber can slide within either a steel cap, with the optical beam passing through one of the slots (b); or within a transparent plastic cover (c). Imaging is performed with the catheter in gentle contact with the esophageal wall (d).

### 2.3 Animal Model

Male Fischer rats with body weights of ~180 grams were anesthetized with ketamine (80 mg/kg) and xylazine (13 mg/kg) administered intramuscularly. Each animal received only water during the day before EDOCT imaging to reduce food debris in the esophagus. The EDOCT catheter was introduced through the mouth into the esophagus. Structural, color-Doppler, and velocity variance mode images were acquired at 1~2 Hz [1,2]. During imaging, the animal's body temperature was maintained by a heating pad. After imaging the animal was sacrificed with the catheter in the esophagus as a marker for the region imaged, which was resected for histology. The procedures were performed in accordance with an institutionally approved animal utilization protocol.

### 2.4 Human Trial

Patients undergoing upper GI endoscopy at St. Michael's Hospital, Toronto, were recruited for the EDOCT feasibility study, with institutional approval and informed consent. EDOCT imaging was performed at the end of the conventional endoscopy procedure with the catheter inserted through the accessory channel. For this feasibility study, esophagi with normal endoscopic appearance were imaged with the catheter in gentle contact with the esophageal wall. No biopsies were obtained since the imaged regions were normal. The EDOCT images were acquired at 1~2 Hz. The catheter was detached and reprocessed (cleaned) using a standard accessory processing protocol between patients.

## 3. Results and discussions

A set of typical EDOCT images of normal rat esophagus is shown in Fig. 4, demonstrating the feasibility for structural, color-Doppler, and velocity variance imaging *in vivo*. A blood vessel of approximately 100  $\mu\text{m}$  in diameter can be seen at the center of the color-Doppler image (which displays the mean Doppler shift frequency) and the velocity variance image (which displays the normalized variance of the Doppler shift frequency). In this example, aliasing can cause the mean Doppler shift to fluctuate randomly from one pixel to the next, as shown in Fig. 4(b), which makes it difficult to visualize the blood flow. On the other hand, blood flow with aliased mean Doppler shifts typically has high variance, as shown in Fig.4(c).

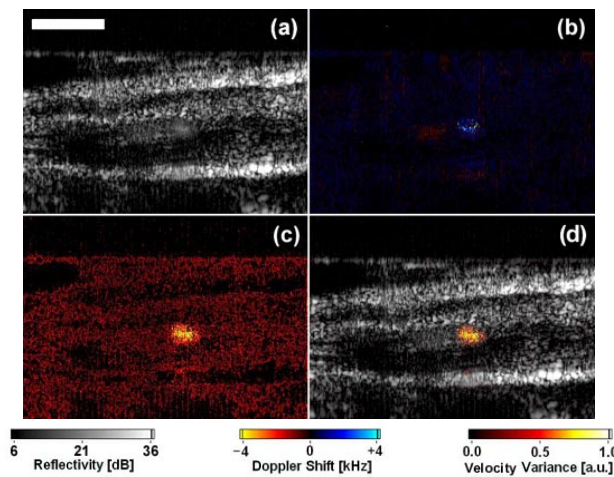


Fig. 4. EDOCT image sequence [289 kB], showing blood flow in a submucosal blood vessel in rat esophagus. Frame acquisition time = 1 second. (a) Structural image. (b) Color-Doppler image showing the mean Doppler shift. (c) Normalized velocity variance image. (d) Composite image with the velocity variance overlaid on the structural image. Bar = 500  $\mu\text{m}$ .

From the rapid up and down fluctuations of the rat esophagus in these images, it is evident that considerable tissue motion can occur during the image acquisition time. This is probably due to the high heart rate of the rat (normally 200 ~ 300 beats per minute). Larger blood vessels can exhibit pulsatile flow, which is better detected in M-mode imaging (displaying structural, color-Doppler, and velocity variance data along a fixed axial direction over time), as shown in Fig. 5. The Doppler frequency spectrum, representing the distribution of flow velocity at a certain depth, was also calculated and presented as an audio output, as described in the companion papers [1,2]. This is shown in Fig.6, where the depth is chosen at the center of the blood vessel. From Fig.5 and 6, the heart rate can be measured as ~214 beats per minute.

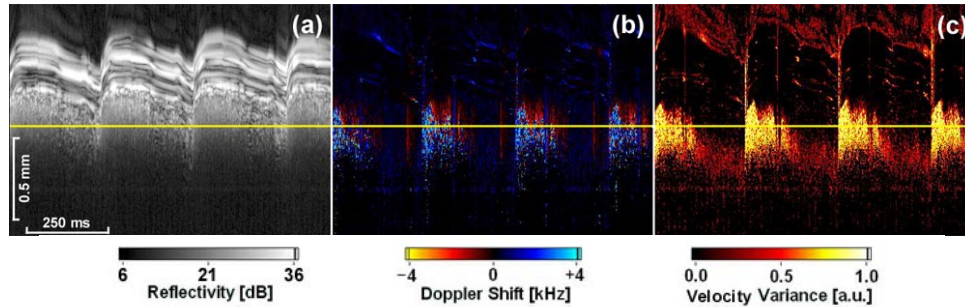


Fig. 5. M-mode EDOCT image showing the pulsatile blood flow in a major blood vessel in the close vicinity of the rat esophagus. (a) Structural image. (b) Color-Doppler image showing the mean Doppler shift. (c) Normalized velocity variance image. The yellow horizontal line indicates the depth from which Doppler spectrum information is processed (see Fig.6).

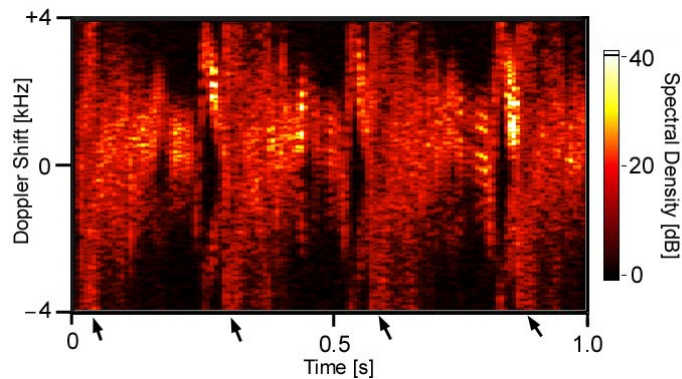


Fig. 6. Doppler spectrum corresponding to Fig.5, demonstrating the EDOCT system's ability to detect the pulsatile blood flow velocity distribution in the rat. High speed blood flow at the beginning of the pulse caused significant aliasing (arrows), consistent with Fig.5(b). The Doppler spectrum is also presented in audio format [393 kB].

Substantial motion can be observed in Fig. 4, which can be better visualized in the structural image if the frame rate is increased to 4 or 8 images per second. However, the noise background in both the mean Doppler shift and velocity variance images increases, as found previously using flow phantoms and tadpole embryos at these frame rates [1,2]. The main causes are increased speckle modulation and mechanical vibrations due to rapid scanning of the sample arm fiber. Hence, for this feasibility study, we limit the frame rate below 2 images per second to maximize the probability in detecting blood flow endoscopically. At 1 to 2 frames per second, the velocity noise background is dominated by the signal-to-noise ratio and electro-mechanical phase stability of the interferometer [1]. The EDOCT images were in agreement with histological examination (results to be published elsewhere).

In the normal human esophagus, more structural features can be identified (see Fig.7.), in agreement with previous non-Doppler OCT studies [5,8]. With the Doppler information overlaid on the structural images, several observations can be made. Closer to the esophagus surface, there is a layer of small blood vessels (diameter  $< 100 \mu\text{m}$ ) in the shallow connective tissue layer (lamina propria). They are probably part of the superficial capillary network and can be detected using the velocity variance images, as shown in Fig.7 (a) and (b). Beneath this layer, a group of larger blood vessels (diameter ranges from 100 to  $400 \mu\text{m}$ ) can be found in the deeper connective tissue layer (submucosa). They can be detected with either velocity variance or color-Doppler images, as shown in Fig.7 (a), (c), and (d). Due to the difficulty in measuring the Doppler angle, absolute velocity of the blood flow is difficult to determine. However, estimation of the minimum or axial velocity is possible. For example, the minimum flow velocity at the center of the large (diameter  $\sim 400 \mu\text{m}$ ) vessel in Fig.7 (c) is approximately  $0.7 \text{ mm/s}$ . This is probably a vein. The streaks below the vein are Doppler artefacts due to multiple scattering of the detected photons. The minimum flow velocity at the center of the small (diameter  $\sim 100 \mu\text{m}$ ) vessel is about  $3 \text{ mm/s}$ . This is probably a small artery.

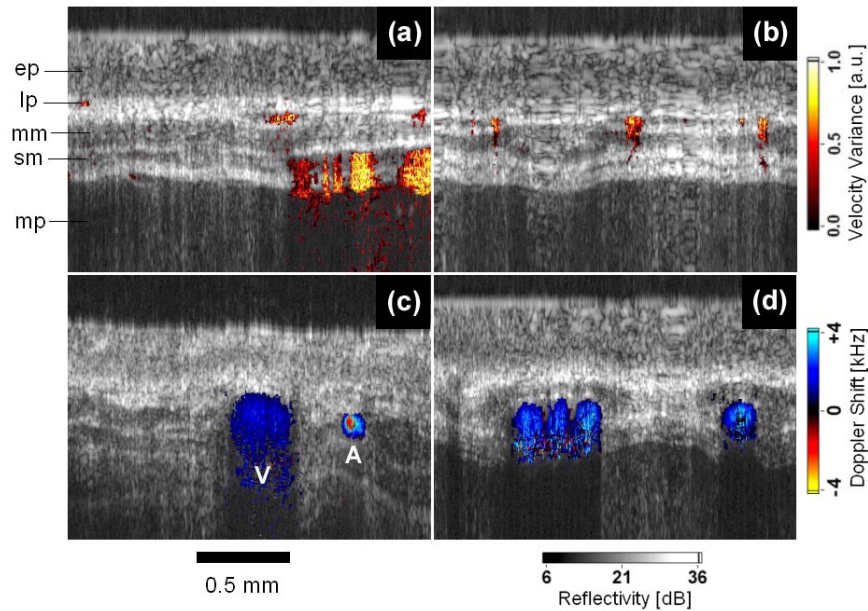


Fig. 7. Example EDOCT images of normal human esophagi from different patients, with the velocity variance information overlaid on the structural images in (a) and (b), and the mean Doppler shift overlaid in (c) and (d). Note the clearly delineated layers of normal esophagus: ep – epithelium, lp – lamina propria, mm – muscularis mucosa, sm – submucosa, and mp – muscularis mucosa. Note the high velocity blood flow in the small vessel in (c), which was probably a small artery (A), as indicated by the aliased color-ring. The adjacent larger vessel is probably a vein (V).

Our limited clinical experience to date has been that the absolute frame rate is not the most important factor, since a structural image overlaid with Doppler flow map contains a lot of information, and the endoscopist needs time to appreciate such details. Our RSOD operating at  $8 \text{ kHz}$  provides the ability to acquire a large number of axial scans. This is important for signal processing to reduce velocity noise. The RSOD allows image acquisition during a short time, which is critical for successful clinical EDOCT imaging by capturing a relatively quiet time-window between heartbeat, breathing, and/or peristalsis. Practically, a near real-time structural OCT display provides helpful visual feedback for the endoscopist to maneuver the catheter, while the Doppler information can be displayed separately for

interpretation. Hence, in the future, a dual-frame-rate system may employ an alternative design similar to Doppler ultrasound where the structural image is captured at higher frame rate than the flow information [15].

For the rat and human esophagus imaging, we tried catheters terminated with both the slotted steel cap and the transparent plastic cover. Experience showed that while, in theory, the slotted cap design should allow better optical performance, in practice it was difficult to align the optical beam during endoscopy such that the cap was not obstructive. The fine angular alignment could be managed in well-controlled settings such as the rat esophagus imaging. However, during clinical endoscopy we found the transparent plastic cover design to be more practical, since angular adjustment of the fiber was coarse at best over the length of the endoscope. The additional optical surfaces in the latter design did degrade image quality slightly, but the practical convenience outweighed this limitation.

To achieve optimal scanning, the required slope and duration of the fast falling portion of the modified saw-tooth driving waveform are related to the length of the endoscope, and the resulting static friction between the sliding fiber and the stationary guiding catheter. In addition, the amount of bending of the endoscope is an important factor. In principle, the entire length of the catheter can use the transparent plastic cover [7], instead of joining the cover to the non-transparent guiding catheter as in our design. We have experimented with this alternative approach. However, the static friction seems to be higher, thus requiring larger amplitudes of the fast pullback motion. This can produce vibrations in the fiber, which can cause the slow pullback motion to be erratic. In addition, since the overall travel of the piston is limited, the end result is reduced lateral scanning range at a given frame rate. The choice of fiber and catheter material, the tolerance of machining and polishing, and the driving waveform all contribute to the mechanical impact on the overall velocity noise in our system. Malfunction in any one of these components will cause sub-optimal system performance, and prevent detection of microcirculation during endoscopy. It is critical that all of these factors are minimized, since phase-resolved optical interferometry is very sensitive to mechanical disturbances [16].

Finally, endoscopic probe designs that do not mechanically stress the fiber may be better suited for EDOCT. Forward-viewing probes using piezo-cantilever actuators [6] that minimally bend the fiber may fulfill the requirements at the present time. In the future, catheters incorporating MEMS (micromachined-electro-mechanical-system) mirrors for beam steering and scanning may prove useful.

As we proposed in the first article [1] of this series, one of our goals was to extend the commonly used Doppler ultrasound techniques into the optical regime, including the display modes of mean Doppler shift frequency, velocity variance, and Doppler frequency spectrum (with audio information). Extending these techniques from the acoustic to optical wavelengths and using interferometric instead of time-of-flight measurements provided up to 100-fold improvement in the velocity sensitivity and resolution compared with ultrasound, as found by a flow phantom study [1]. The improved velocity resolution allowed novel methods for separating the blood-flow velocity from motion artefacts, such as the histogram segmentation algorithm that we developed [1,12]. This enabled detection of blood flow velocities that were slower than the surrounding tissue motion, which had been challenging in Doppler ultrasound that often used high-pass filters [15]. Using these techniques and a hand-held scanner, the second article [2] demonstrated the capability of imaging dynamic blood flow at high speed (4-16 frames per second), using the tadpole heart as a model. The hand-held scanner optics was intentionally designed as a "proof-of-principle" for the endoscopic catheters used in this final study of endoscopic applications. Thus, we have systematically extended commonly used Doppler ultrasound techniques to OCT in hand-held and endoscopic configurations, for detection and imaging of microcirculation.

#### 4. Conclusions

In conclusion, we have demonstrated an *in vivo* endoscopic Doppler OCT system capable of imaging subsurface microcirculation in the rat and human GI tracts. Specialized mechanical



and optical components of the system, in addition to electronics and digital signal processing designs, allowed clear microstructural delineation of the esophagus and the detection of microvascular distribution in the esophageal wall. Using this system, microvascular flow in blood vessels less than 100  $\mu\text{m}$  diameter was imaged in the esophagus, employing a combination of color-Doppler, velocity variance and Doppler spectrum display modes. We are currently exploring the scientific and clinical implications of these results. To our knowledge, this is the first demonstration of endoscopic Doppler OCT under normal clinical conditions.

### **Acknowledgement**

This work was supported by the Natural Sciences and Engineering Research Council of Canada, the Canadian Institutes for Health Research, the Canadian Cancer Society through a grant from the National Cancer Institute of Canada, the Canadian Foundation for Innovation, Photonics Research Ontario, and a donation from the Gordon Lang Foundation. The authors would like to thank M. Filleti, Machine Shop, Princess Margaret Hospital, Toronto, for the fabrication work. We are grateful to the clinical support provided by M. Cirocco and N. Basset, St. Michael's Hospital, Toronto. We also acknowledge the experimental assistance of N. Swoboda. Discussions with Drs. G. J. Tearney and J. de Boer, Wellman Laboratory of Photomedicine, Massachusetts General Hospital, regarding the linear scanner, were appreciated. Discussions with Drs. Z. Chen and Y. Zhao, Beckman Laser Institute, University of California, Irvine, regarding the optical Doppler tomography technique, were also appreciated.